Lysine demethylase 2A promotes the progression of ovarian cancer by regulating the PI3K pathway and reversing epithelial-mesenchymal transition

DAN-HUA LU[1], JIANG YANG[1], LI-KUN GAO[1], JIE MIN[1], JIAN-MING TANG[1], MING HU[1], YANG LI[1], SU-TING LI[1], JING CHEN[2] and LI HONG[1]

[1]Department of Gynaecology and Obstetrics, Renmin Hospital of Wuhan University, Wuhan, Hubei 430060, P.R. China; [2]Department of Pathology, Molecular Diagnostics Laboratory, University of Michigan, Ann Arbor, MI 48109, USA

Received June 4, 2018; Accepted November 21, 2018

DOI: 10.3892/or.2018.6888

Abstract. Metastasis is the most common cause of death in ovarian cancer patients but remains largely untreated. Epithelial-mesenchymal transition (EMT) is critical for the conversion of early-stage ovarian tumors into metastatic malignancies. Thus, investigating the signaling pathways promoting EMT may identify potential targets for the treatment of metastatic ovarian cancer. Lysine demethylase 2A (KDM2A), also known as FBXL11 and JHDM1A, is a histone H3 lysine 36 (H3K36) demethylase that regulates EMT and the metastasis of ovarian cancer. However, the function and underlying mechanisms of EMT suppression in ovarian cancer have not been thoroughly elucidated to date. In the present study, we used Gene Expression Omnibus (GEO) databases to determine that KDM2A is significantly upregulated in human ovarian cancers. KDM2A expression was assessed by immunohistochemistry of epithelial ovarian cancer (EOC) borderline ovarian tumors and normal ovary tissues. Seven fresh EOC tissues and 3 fresh normal ovary tissues were collected for western blot analysis. Kaplan-Meier survival curves were constructed to identify genes related to EOC prognosis from the TCGA data portal. Stable KDM2A-knockdown cell lines were established to study the biological functions and underlying mechanisms of KDM2A in EMT *in vitro*. GEO database analysis revealed that KDM2A was highly upregulated in EOC tissues; this analysis was accompanied by immunochemistry and western blot analysis using samples of human tissues. High expression of KDM2A was associated with poor survival in EOC patients. KDM2A knockdown promoted apoptosis and suppressed the proliferation, migration and invasion of tumor cells *in vitro*. EMT and the PI3K/AKT/mTOR signaling pathway were suppressed in KDM2A-silenced cells. Inactivation of the PI3K/AKT/mTOR signaling pathway in A2780 cells induced EMT inhibition. Our data revealed that KDM2A functions as a tumor oncogene, and the downregulation of KDM2A expression regulates EMT and EOC progression, providing a valuable prognostic marker and potential target for the treatment of EOC patients.

Correspondence to: Professor Li Hong, Department of Gynaecology and Obstetrics, Renmin Hospital of Wuhan University, 9 Zhangzhidong Road, Wuchang, Wuhan, Hubei 430060, P.R. China
E-mail: drhongli777@163.com

Key words: ovarian cancer, lysine demethylase 2A, tumor spread, epithelial-mesenchymal transition, prognosis

Introduction

Ovarian cancer is the second most common gynecological cancer and currently ranks as one of the leading causes of cancer-related deaths among women worldwide (1,2). Epithelial ovarian cancer (EOC) is the most common and lethal type of the disease, which accounts for approximately 85-95% of all ovarian cancer cases. EOC treatment commonly results in a low response rate to surgical resection, radiotherapy, chemotherapy and poor prognosis with a median survival of <5 years in approximately 30% of patients (3,4). The high morbidity and mortality rates are contributed to the fact that patients may appear asymptomatic in the early stages; therefore, 70-75% of patients in the advanced stages are often diagnosed after the cancer has circulated throughout the abdominal cavity (5,6). Therefore, a rapidly expanding understanding of the molecular mechanisms underlying the pathogenesis of EOC, especially the mechanisms that affect OC cell invasive, has the potential to strongly influence treatment outcomes for this devastating disease.

The histone H3 lysine 36 demethylase enzyme (KDM2A) has been previously shown to demethylate histone H3K36, contain an F-box domain, a JmjC domain, a CxxC zinc finger domain, a PHD domain and 3 leucine-rich repeat elements belonging to the KDM gene family (7-9). KDM2A was first discovered in kidney COS-7 cells exhibiting robust histone demethylase activity (10). KDM2A was found to be highly expressed in lung (11), pancreatic cancer (12), colorectal adenocarcinoma (13), breast (14), gastric cancer (15) and certain blood diseases (16), which have been reported to be

related to tumor aggressiveness and metastasis, chemotherapy resistance and poor prognosis. This protein has been linked to many signaling pathways, which promote cancer metastasis and malignancy. Wagner *et al* showed that KDM2A promoted lung tumorigenesis via the ERK1/2 signaling pathway (11). Chen *et al* reported that KDM2A promoted angiogenesis and stemness by upregulating Jagged1 (17). However, the role of KDM2A and its underlying mechanism still remain unclear in EOC proliferation, migration and metastasis. In the present study, we demonstrated that KDM2A is overexpressed in EOC and that KDM2A promoted EOC progression and induced EMT. Furthermore, KDM2A influenced the biological behaviors previously mentioned by regulating the PI3K/AKT/mTOR pathway. These findings suggest that KDM2A may serve as a potential therapeutic target for the clinical management of EOC.

Materials and methods

Bioinformatic analysis. Gene profiling data of ovarian normal surface epithelia and ovarian cancer epithelial samples were downloaded from the GEO dataset (http://www.ncbi.nlm.nih.gov/geo). GSE14407 dataset was selected for bioinformatic analysis (18). The differential analysis was performed using R package 'limma' (19). Differential genes obtained from GSE14407 were visualized using the R package 'pheatmap' (https://CRAN.R-project.org/package=pheatmap) and 'ggplot2' (20). RNA sequencing data of KDM2A was achieved from the TCGA data portal (https://cancergenome.nih.gov/), containing 374 ovarian cancer samples. Corresponding clinical data were also downloaded and filtered out for useful information. Kaplan-Meier survival curves were conducted to assess the prognostic value of KDM2A using the R package 'survival' (https://CRAN.R-project.org/package=survival).

Ovarian cancer tissue samples. Human specimens were obtained between 01 January 2005 and 31 December 2011 from 27 patients, with a mean age of 46 years (range, 18-73 years), who underwent primary tumor resection at Renmin Hospital of Wuhan University (Wuhan, China). Among the 27 cases, the specimen groups consisted of EOC (n=9), borderline ovarian tumors (n=9) and normal ovary tissues (n=9). All specimens were confirmed by at least 2 pathologists. In the present study, the patients accepted no chemotherapy or radiotherapy before surgery. Before conducting our scientific investigation, consent was obtained from all the patients and the study was approved by the Ethics Committee of Wuhan University (Wuhan, China).

Immunohistochemistry. The immunohistochemical analysis of KDM2A expression in human EOC was performed as previously described (21). The rate of KDM2A-positive cells was scored semi-quantitatively in each section.

Cell culture and reagent. The human OC cell lines A2780 and SKOV3 were obtained from the State Key Laboratory of Molecular Biology, Institute of Biochemistry and Cell Biology, Shanghai Institutes for Biological Sciences, Chinese Academy of Sciences (Shanghai, China). The cells were respectively cultured in MEM/F12 and RPMI-1640 medium supplemented with 10% fetal bovine serum (FBS) (both from Gibco; Thermo Fisher Scientific, Inc., Waltham, MA, USA), 1% penicillin and 1% streptomycin (Sigma-Aldrich; Merck KGaA, Darmstadt, Germany) in a CO_2 incubator under standardized conditions. Antibodies KDM2A (cat. no. ab191387), GAPDH (cat. no. ab181602), and β-actin (cat. no. ab8227) were obtained from Abcam plc. (dilution 1:500; Cambridge, UK). Antibodies phospho-PI3K (cat. no. sc4257), PI3K (cat. no. sc4292), phospho-Akt (cat. no. sc4060), Akt (cat. no. sc4691), phospho-mTOR (cat. no. sc5536), mTOR (cat. no. sc2983), MMP2 (cat. no. sc10736), MMP9 (cat. no. sc10737), Bcl-2 (cat. no. sc2872), Bax (cat. no. sc14796), E-cadherin (cat. no. sc14472), N-cadherin (cat. no. sc13116) and vimentin (cat. no. sc5741) were purchased from Cell Signaling Technology (dilution 1:500; Danvers, MA, USA). LY294002 was reported as the inhibitor of the PI3K, which was purchased from Nanjing KeyGen Biotech Co., Ltd. (Nanjing, China) (22).

Establishment of the stable KDM2A-knockdown cell line Transfection. In order to knockdown the expression of endogenous KDM2A, a lentivirus containing an shRNA sequence targeting KDM2A was designed and synthesized by Shanghai GenePharma Co., Ltd. (Shanghai, China). The shRNA sequence was as follow: GGTGGGCAGTAGGAATCAA. The cells were seeded at ~$1.0x10^5$ cells/well into 6-well plates and cultured at 37˚C overnight under standard conditions. After 50% confluence was reached, the number of cells in a well was counted using a hemocytometer. KDM2A shRNA was transfected into the cells in Opti-MEM (Invitrogen; Thermo Fisher Scientific, Inc.) at a multiplicity of infection (MOI) of 10 [MOI = transducing units per cell (TU) number/cells], according to the manufacturer's instructions. The culture medium was replaced after a 24-h incubation. A total of 48 h after transfection, the cells were observed and photographed under a fluorescence microscope. After successful transfection, the shRNA sequence was stably expressed. Untransfected cells were used as a blank control, while cells transfected with scrambled shRNA were considered as the negative control (shControl).

Cell viability assay. Cell Counting Kit-8 (CCK-8; purchased from Dojindo Laboratories, Kumamoto, Japan) was used to determine the inhibitory effect of the silencing of KDM2A on the proliferation of A2780 and SKOV3 cell lines according to the manufacturer's instructions. Cells were seeded at ~$10.0x10^3$ cells/well into 96-well plates with 10% FBS and cultured for 24, 48 and 72 h. Then, 10 μl of CCK-8 was added and subsequently incubated for 1 h at 37˚C. The absorbance value (OD) at 450 nm of every well was measured with a spectrophotometric plate reader. Assays were performed in triplicate on 3 independent experiments.

Colony formation assay. An appropriate number of cells were plated on a 6-well plate (500 cells/2 ml/well) and cultured in 2 ml medium with 10% FBS. Then, cells were changed every 3 days with 10% mycoplasma-free FBS for 2 weeks until the cells in the plates had formed colonies that were of substantially right size (50 cells/colony or greater). The cells were fixed with 2 ml 75% ethanol at room temperature for 15 min, and then stained with 0.5% crystal violet. The cloning efficiency was

calculated by dividing the number of wells containing proliferating cells with the total number of cell-plated wells.

Flow cytometric analysis of apoptosis with PE/7-ADD staining. For apoptosis analysis, cells were treated for 48 h. The cells were suspended with 100 μl of 1X binding buffer (0.1 mM HEPES/NaOH, 1.4 M NaCl, 25 mM $CaCl_2$ and pH 7.4) and stained with 5 μl of PE Annexin V and 5 μl of 7-amino-actinomycin (7-ADD) for 15 min at room temperature and then 400 μl 1X binding buffer was added to each tube (Annexin V-PE Apoptosis Detection kit; BD Pharmingen; BD Biosciences, San Diego, CA, USA). Analysis of the results was carried out by BD FACSAria (BD Biosciences, Franklin Lakes, NJ, USA). Data were quantified using FlowJo Software (FlowJo, LLC, Ashland, OR, USA).

Hoechst staining. The 3 groups of A2780 and SKOV3 cells were fixed using methanol acetic acid for 15 min and then stained with Hoechst 33342 for 5 min. Being washed twice with PBS, the cells were immediately photographed under an Olympus BX51 inverted microscope at x400 magnification (Olympus Corp., Tokyo, Japan).

Wound healing assay. Untransfected and transfected cells were seeded at $5.0x10^5$ cells/well in 6-well plates and cultured routinely. After reaching 90% confluence, the cell monolayer was scratched with a sterile pipette tip. After washing 3 times with PBS for 5 min each to clear the floating cells, 1.5 ml MEM/F12 and RPMI-1640 medium supplemented with 1% FBS were added into each well. Photographs were taken by an Olympus BX51 inverted microscope at x100 magnification (Olympus Corp.) at 0, 24 and 48 h after scratching. Results were indicated as the relative width of scratch-the distance migrated relative to the original scratched distance. The experiment was conducted 3 times.

Cell invasion assay. The invasive ability of cells was measured using the Corning® Matrigel® Basement Membrane Matrix (cat. no. 356234; Corning Inc., Corning, NY, USA) and a 24-well Transwell chamber (Corning Inc.) according to the manufacturer's protocol. The number of cells that passed through an 8-μm polycarbonate membrane was calculated. The polycarbonate surface of each chamber was covered with 50 μl Matrigel (1:8 dilution) to create an artificial basement membrane. Cells were cultured at 37˚C in FBS-free MEM/F12 and RPMI-1640 medium for 24 h. After serum starvation, the cells were seeded at $1x10^5$ cells/well in the upper Transwell chamber, which contained ~200 μl serum-free medium. The lower chamber was filled with 500 μl of the medium supplemented with 10% FBS. After an incubation of 48 h at 37˚C, the chambers were fixed at room temperature with paraformaldehyde for 30 min. Cells that had attached to the upper surface of the chambers were removed with a sterile cotton swab, and cells that adhered to the lower surface were stained with 0.1% crystal violet (Guangfu Institute of Superfine Chemical Industry, Tianjin, China) for 20 min at room temperature. The numbers of stained cells were counted using an inverted microscope (Olympus IX 70-142; Olympus Corp.) in 8 random fields. The experiment was repeated 3 times.

Western blot analysis. Cell lysates containing equal amounts of protein was subjected to 12% SDS-PAGE and then transferred to 0.45 μm Immobilon-P transfer membranes (EMD Millipore, Billerica, MA, USA) by electroblotting. Membranes were blocked at room temperature for 1 h in TBST (50 mmol/l Tris-HCL, pH 7.6, 150 mmol/l NaCl and 0.1% Tween-20) containing 5% non-fat dry milk and then incubated with primary antibody at 4˚C overnight. The membranes were then incubated with appropriate anti-rabbit secondary antibody (dilution 1:10,000; Sigma-Aldrich; Merck KGaA) for 1 h at room temperature and visualized with a chemiluminescence substrate kit (Pierce™ ECL Western Blotting Substrate; Thermo Scientific Fisher, Inc.). The intensity of the target protein bands was normalized to the loading control, GAPDH/β-actin.

Statistical analysis. Statistical analyses were performed using SPSS v. 17.0 software (SPSS, Inc., Chicago, IL, USA). Quantitative data are expressed as the mean ± standard deviation (SD). The log-rank test, one-way ANOVA and and the Tukey's test were used. The statistically significant difference was indicated in the figures and legends as follows: $^{*}P<0.05$, $^{**}P<0.01$, $^{***}P<0.001$.

Results

KDM2A is upregulated and associated with poor survival in EOC. Differential analysis was performed for the GSE14407 dataset. The results showed that expression of KDM2A was significantly upregulated in 12 serous ovarian cancer epithelial samples (SOCE) compared to that noted in the 12 healthy ovarian surface epithelial samples (HOSE) (Fig. 1A and B). Differences in the immunoreactivity of KDM2A staining were observed in EOCs, borderline epithelial ovarian tumors, and normal epithelial ovary tissues, predominantly expressed in the nucleus and light cytoplasmic staining. EOCs showed strong positive staining, while borderline epithelial ovarian tumors and normal ovary tissues showed low-level expression (Fig. 1C). Kaplan-Meier survival analysis suggested that patients with high KDM2A expression had a poor prognosis in overall survival (Fig. 1D). In addition, the expression level of KDM2A was higher in 7 fresh EOC tissues compared with that in 3 fresh normal ovary tissues (Fig. 1E).

Assessment of KDM2A expression after shRNA transfection. To test the function of KDM2A in EOCs, shRNA transfection was used for KDM2A knockdown. The knockdown efficiency was assessed by western blot analysis. The results showed that the expression of KDM2A was significantly decreased after shRNA-KDM2A transfection in human ovarian cancer cell lines SKOV3 and A2780 (Fig. 2A and B).

Silencing of KDM2A reduces proliferation and delays G2 phase progression. We found that KDM2A inhibition in A2780 and SKOV3 cells prevented proliferation. We tested our hypothesis to confirm whether cell viability and the colony-forming capabilities were determined by cell proliferation. As shown in Fig. 2C, CCK-8 was used to measure the viability of EOC cells transfected with sh-KDM2A. The viability of the sh-KDM2A cells was significantly lower than that for cells transfected with

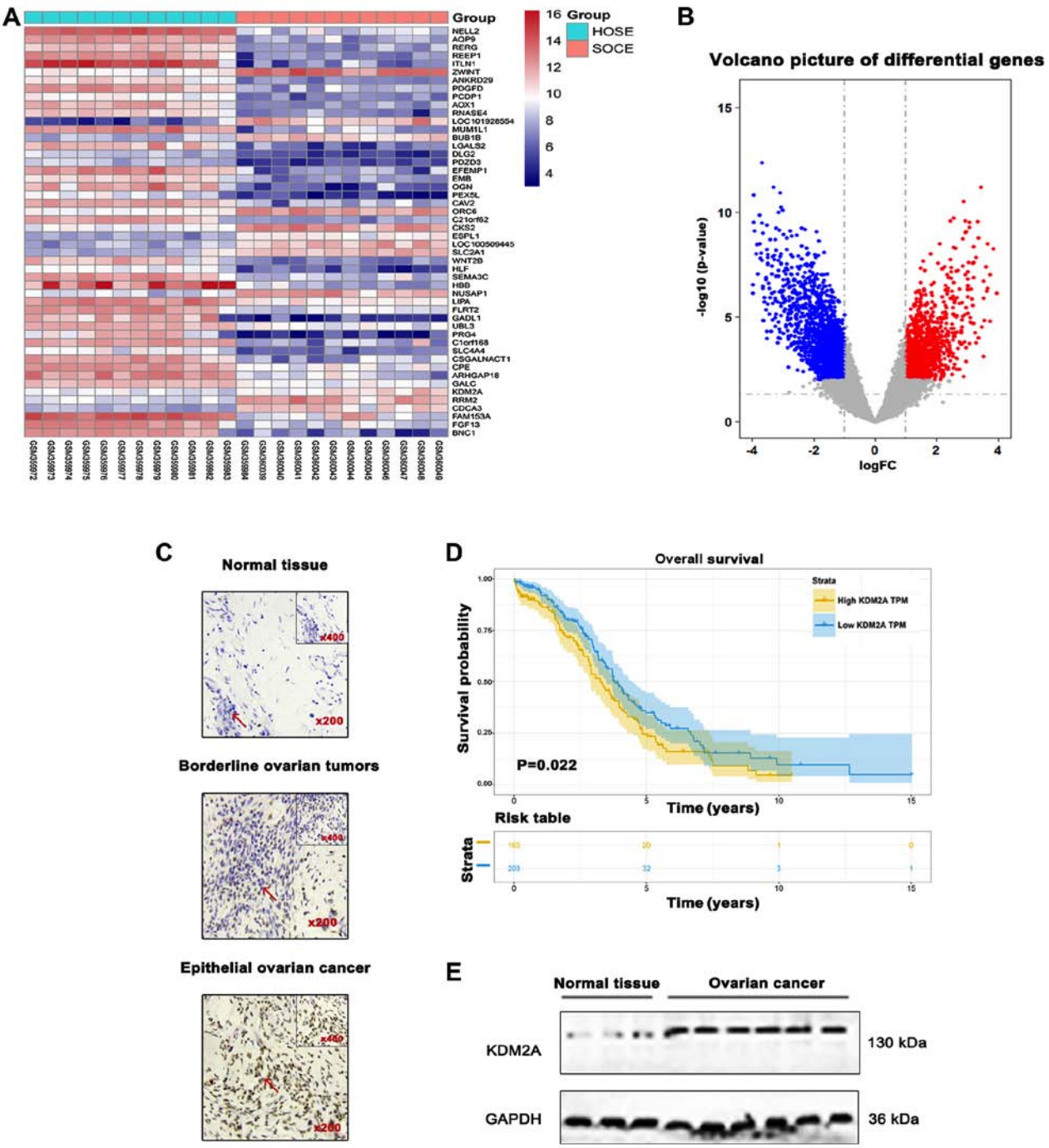

Figure 1. KDM2A expression in EOC tissues. (A) Differential genes obtained from the GSE14407 dataset were visualized using a (A) heatmap and (B) volcano plot. (C) Representative immunohistochemical staining of KDM2A in representative EOC tissues and normal ovarian epithelia. The inset is a zoomed image. Original magnification, x200. Scale bars, 50 μm. (D) The overall survival curves of patients with KDM2A-low and -high indices. A significant difference was observed between groups (P=0.022). (E) The expression level of KDM2A was higher in 7 fresh EOC tissues compared with 3 fresh normal ovary tissues. EOC, epithelial ovarian cancer.

the sh-Control and the control group. The colony formation assay indicated that the colony-forming capabilities of the SKOV3 and A2780 cells were significantly impaired due to KDM2A depletion (Fig. 2D). To explore whether the effects of KDM2A depletion on cell behaviors were related to cell cycle distribution, we performed flow cytometric analysis. The evidence showed that the cell cycle was related to the proliferative capabilities of cells; therefore, the effect of KDM2A in EOC was further investigated. The percentage of G2/M phase cells was increased after silencing of KDM2A (Fig. 2E and F). These results demonstrated cell cycle arrest in the G2/M transition due to KDM2A knockdown.

Downregulation of KDM2A stimulates cell apoptosis. Flow cytometric analysis with PE/7-ADD staining showed that the early apoptotic cell population in the sh-KDM2A group was higher than that in the other 2 groups in the 2 cell lines (Fig. 3A and B). Moreover, western blot analysis showed that the expression level of Bcl-2 was downregulated, while the expression level of Bax was upregulated in the same

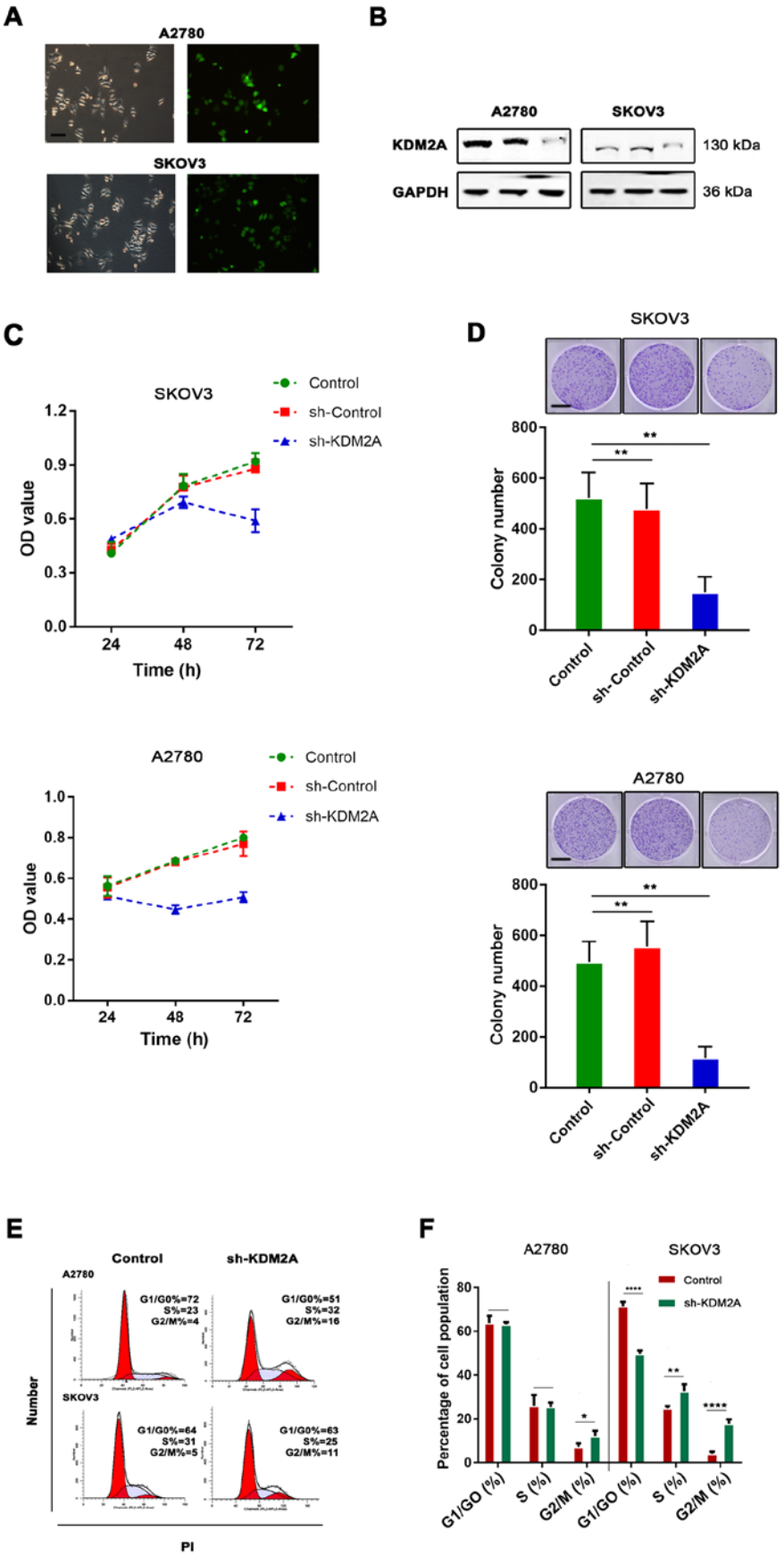

Figure 2. Effects of KDM2A on EOC cell proliferation. (A and B) shKDM2A was introduced into SKOV3 and A2780 cells, and the silencing efficacy was confirmed by western blot analysis. Scale bar, 50 μm. (C) Cell viability was determined by CCK-8 assay after shKDM2A knockdown treatment at various time-points (24, 48 and 72 h) in SKOV3 and A2780 cells. (D) KDM2A knockdown reduced the ability of colony formation of SKOV3 and A2780 cells. Scale bar, 100 μm. (E and F) Cell cycle distribution analysis by flow cytometry. KDM2A arrested G2 progression delay. Data are presented as the mean ± SD of at least 3 independent experiments. *P<0.05, **P<0.01, ****P<0.0001, compared with the untreated controls (Control) and the negative controls (sh-Control). EOC, epithelial ovarian cancer.

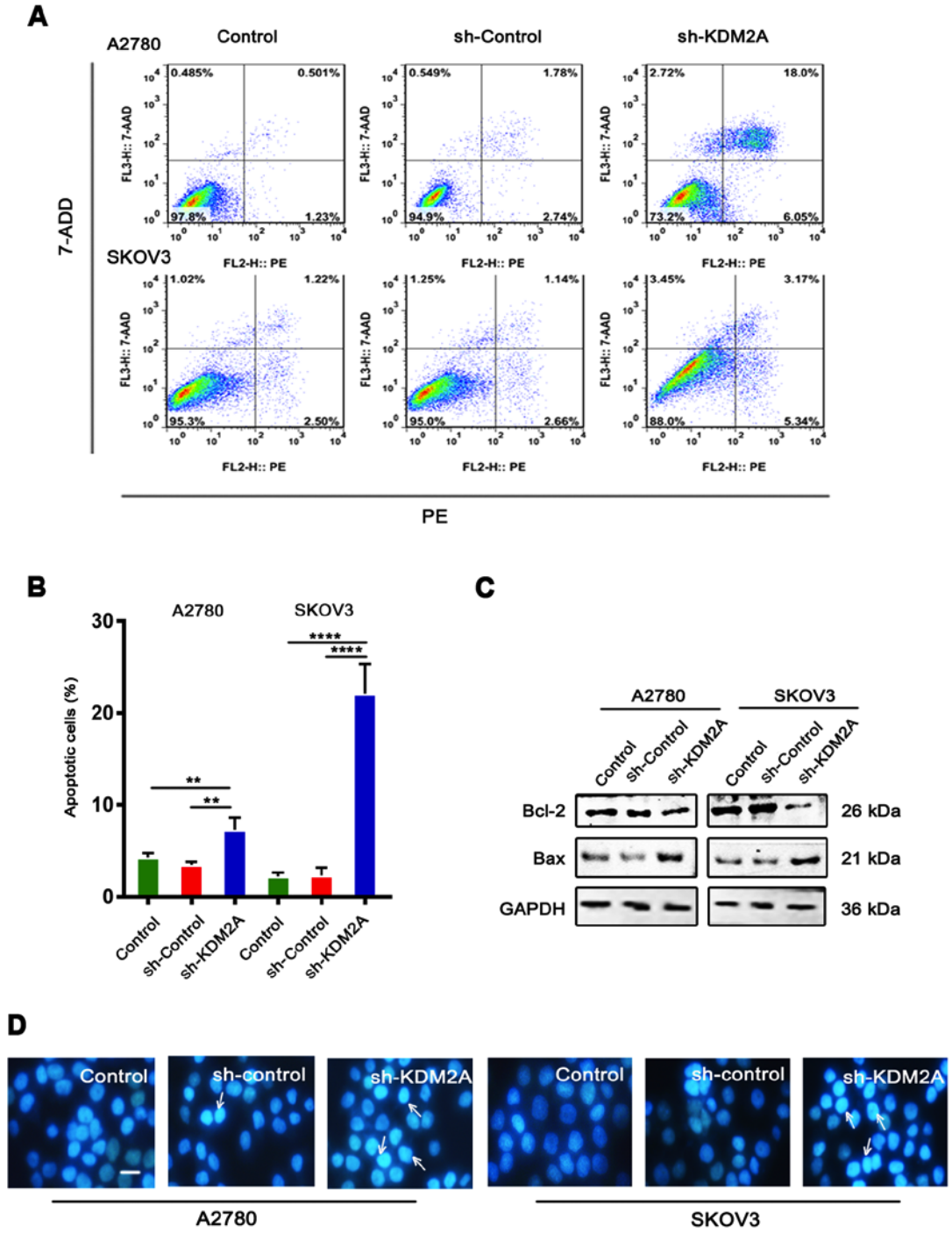

Figure 3. KDM2A silencing increases cell apoptosis. (A and B) Flow cytometric analysis of PE/7-ADD-stained A2780 and SKOV3 cells after transfection. (C) Bax protein was upregulated and Bcl-2 protein was downregulated after transfection. (D) Downregulation of KDM2A increased the apoptosis rate of the A2780 and SKOV3 cells as detected by Hoechst 33342 staining. Scale bar, 20 μm. **P<0.01, ****P<0.0001.

conditions (Fig. 3C). Hoechst 33342 staining showed that the sh-KDM2A group had a greater number of apoptotic cells compared to the number of apoptotic cells in the 2 control groups (Fig. 3D). Additionally, cells of the sh-KDM2A group showed marked morphological changes in the nuclear size than cells of the control groups.

Inhibition of KDM2A attenuates tumor migration and invasion in vitro. The serum-stimulated Matrigel invasion assay demonstrated that the percentages of human ovarian cancer cells that migrated through the polycarbonate membrane in the sh-KDM2A transfection group were significantly lower than those in the control groups (Fig. 4A and B). Therefore, downregulation of KDM2A decreased cell invasion of the human ovarian cancer cell lines after transfection.

The monolayer wound healing assay was used to assess cell migration. The transfected cells showed a significant deceleration in closure of the wound scratch width after 24 and 48 h compared with the sh-Control and control groups (Fig. 4C and D).

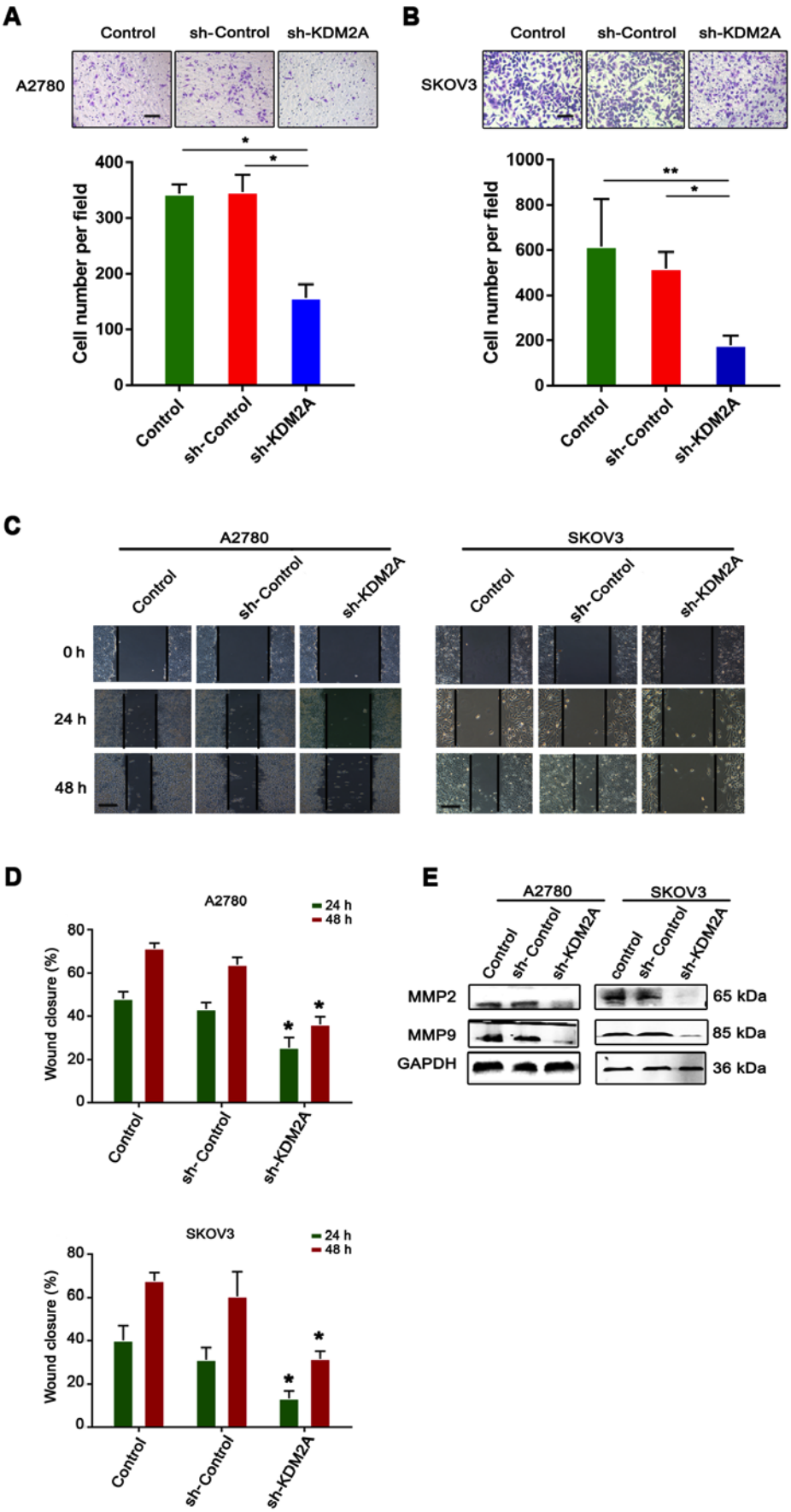

Figure 4. Downregulation of KDM2A suppresses cell migration and invasion of the A2780 and SKOV3 cells. (A and B) The 3 cell groups were collected and assayed for their capabilities of invasion using a Transwell system. Cell invasion of the sh-KDM2A was significantly decreased compared to the 2 control groups. Scale bar, 50 μm. (C and D) The 3 cell groups were calculated for cell migration using the wound healing assay. Cells in the sh-KDM2A group had decelerated scratch wound healing ability. Scale bar, 50 μm. (E) Western blot analysis was used to assess the changes in MMP2 and MMP9 in the 3 groups. The levels of both proteins were decreased in the sh_KDM2A groups. *P<0.05, **P<0.01.

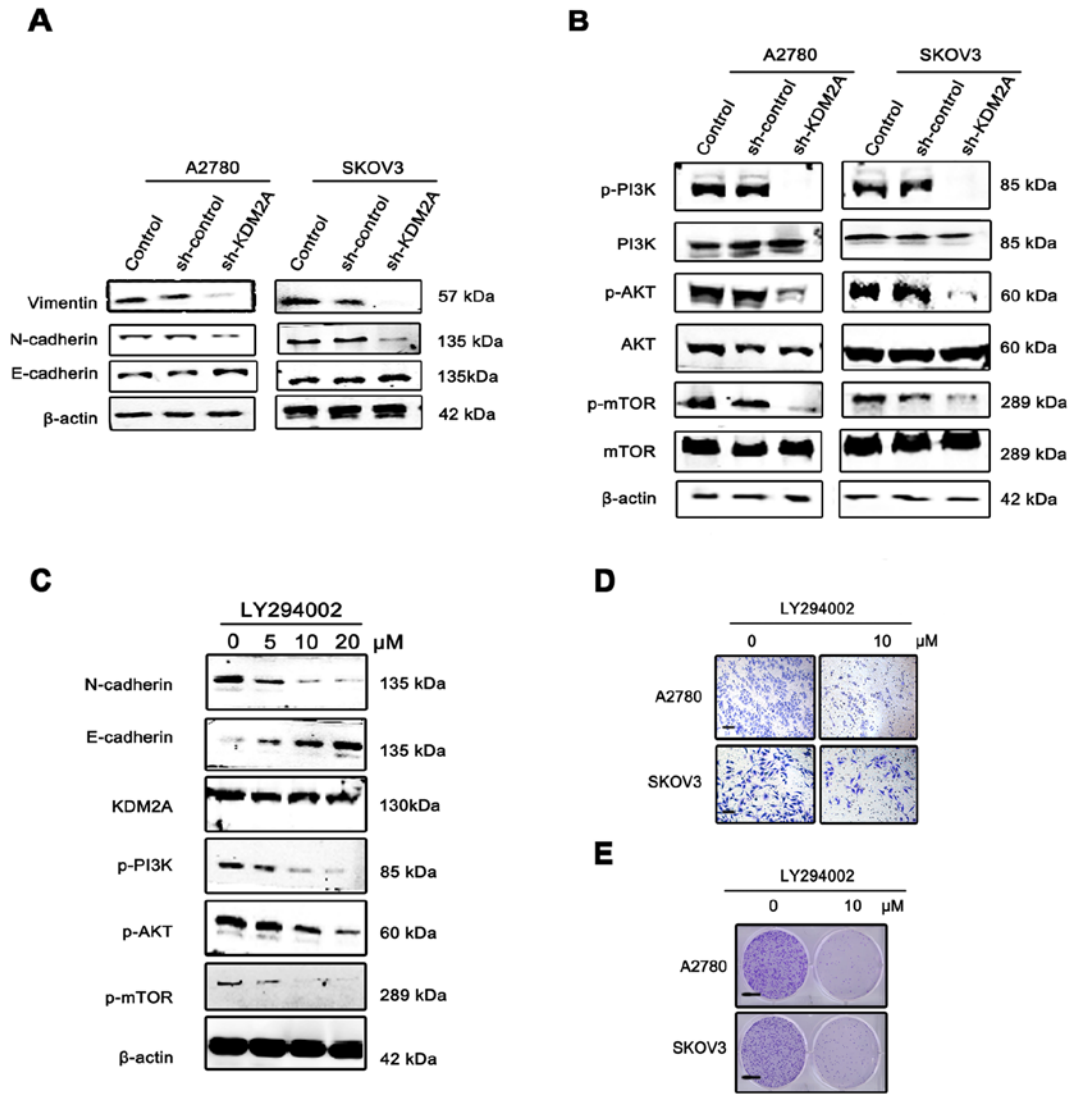

Figure 5. KDM2A facilitates cancer cell EMT via the PI3K/AKT/mTOR pathway. (A) Expression of E-cadherin, N-cadherin and vimentin, EMT phenotype markers, in KDM2A-knockdown cells and the 2 control groups. (B) Activation of the PI3K/AKT/mTOR pathway in the 3 groups. (C) Expression of KDM2A, the EMT phenotype and proteins of the PI3K/AKT/mTOR pathway in A2780 cells were administered gradient concentrations of the PI3K inhibitor (LY294002, 0, 5, 10 and 20 μmol/l). (D) The migration ability of SKOV3 and A2780 cells gradually decreased with 10 μmol/l LY294002. Scale bar, 50 μm. (E) LY294002 inhibited the colony formation of SKOV3 and A2780 cells. Fewer colonies were formed in the treated group compared with the control group. EMT, epithelial-mesenchymal transition. Scale bar, 100 μm.

To study the effect of KDM2A depletion on cellular response, the expression of MMP2 and MMP9 were measured in SKOV3 and A2780 cell lines. As shown in Fig. 4E, the 2 transfected proteins, showed decreased expression in the sh-KDM2A group compared to the negative control and the control group.

KDM2A promotes epithelial-mesenchymal transition (EMT) via the PI3K/AKT/mTOR signaling pathway using the LY294002 in EOC cells. Since EMT has been increasingly recognized as a crucial event in cancer metastasis, we measured the expression of EMT markers and EMT transcription factors before/after KDM2A knockdown by western blotting. The expression level of E-cadherin was markedly upregulated, while those of N-cadherin and vimentin were significantly decreased in A2780 sh-KDM2A and SKOV3 sh-KDM2A cells compared with the sh-Control and the control cells (Fig. 5A).

To elucidate the molecular mechanism involved in KDM2A-mediated EMT in EOC cells, we analyzed the key components of the PI3K/AKT/mTOR signaling pathway. Western blot analysis showed that KDM2A knockdown decreased the expression of phospho (p)-PI3K, p-AKT and p-mTOR compared to the control groups (Fig. 5B). Using the PI3K signaling pathway inhibitor, LY294002 (0, 5, 10 and 20 μmol/l), we treated the A2780 and SKOV3 cells for 48 h. The results showed that inactivation of the PI3K signaling pathway led to suppression of EMT in a dose-dependent manner, while the expression level of KDM2A was not significantly changed (Fig. 5C). The migration ability of SKOV3 and A2780 cells gradually decreased with 10 μmol/l LY294002 (Fig. 5D). In addition, LY294002 inhibited the colony formation of SKOV3 and A2780 cells. Fewer colonies were formed in the treated group compared with the control group (Fig. 5E).

Discussion

In the present study, our results indicated the critical roles of KDM2A in epithelial ovarian cancer (EOC). The significant increase of KDM2A expression in EOC was determined by the GEO database. Similarly, immunohistochemical analysis and western blot analysis confirmed the overexpression of KDM2A in EOC patients compared with the borderline ovarian tumor and normal ovary tissues. Moreover, the Kaplan-Meier estimate showed that KDM2A expression was negatively associated with patient survival, indicating that higher KDM2A expression was correlated with lower overall survival rates of patients with EOC.

To further examine the role of KDM2A in EOC, we investigated the effect of KDM2A on the viability of EOC cells *in vitro*. The results showed that knockdown of KDM2A expression in EOC cells significantly decreased cell proliferation and efficiency of colony formation. In agreement with our findings, KDM2A functions as an oncogene in several types of cancer and several cancer cell lines possess high-level expression of KDM2A (23). Many researchers have concluded that KDM2A may be a promising target in anticancer therapeutics. Huang *et al* showed that forced expression of KDM2A increased the growth and motility of gastric cancer cells by downregulating PDCD, a known tumor suppressor (24). Kong *et al* reported that miR-29b and KDM2A are involved in the proliferation and metastasis of gastric cancer cells (15). Consistent with this finding, KDM2A showed a similar effect on cell apoptosis in this study. We showed that downregulation of KDM2A decreased cell migration and invasion *in vitro*, suggesting that KDM2A promotes EOC tumor metastasis. Hematogenous intravasation and extravasation are less accepted as a mechanism of EOC metastasis. Instead, when cells reach a threshold value, limited by epithelial-mesenchymal transition (EMT) or EMT-like events and growth, a primary OC would passively shed cells from their original location, leading to spheroid formation and formation of peritoneal implantation metastasis (6,25,26).

EMT is a morphological change of cells or tissues that lose their epithelial characteristics and gain mesenchymal properties. EMT is the mechanism that has been well-characterized for the transition of early-stage ovarian cancers to invasive and metastatic malignancies, promoting the aggressiveness of ovarian cancers and obtaining the characteristics of stem cells after a loss of cell polarity and cell-cell adhesion (27-29). Cells undergoing EMT exhibit loss of E-cadherin and increased N-cadherin or vimentin expression, leading to tumor cell invasion and metastasis. E-cadherin is responsible for cell-cell adhesion (30,31); its loss is associated with tumor invasion, metastasis and poor prognosis (32,33). In addition, N-cadherin or vimentin controls tumor progression (34,35). There is sufficient evidence supporting the opinion that the development of EMT in ovarian cancer causes aggressive phenotypes that may promote metastasis (34). Liu *et al* demonstrated that β-hCG-depleted SKOV3 cells had increased E-cadherin and decreased vimentin and N-cadherin expression (36). In addition, Colomiere *et al* demonstrated that expression of mesenchyme-associated N-cadherin and vimentin was consistent with the change in fibroblast-like morphology and migratory phenotype (37). Unsurprisingly, these results confirmed our hypothesis. In this study, we demonstrated that silencing of KDM2A suppressed the EMT process by increasing the expression level of the epithelial marker, E-cadherin, while reducing the mesenchymal markers, N-cadherin and vimentin *in vitro*. These data suggest that KDM2A promotes cancer cell invasion and migration via activation of EMT.

EMT is regulated by various signaling pathways, including the Wnt/β-catenin, Notch, TGF-β and PI3K/AKT signaling pathways (38). Activation of the PI3K/AKT pathway is universal in many malignancies and is associated with carcinogenesis of all ovarian cancer subtypes (39,40). In this study, silencing of KDM2A downregulated levels of phospho-PI3K, phospho-AKT and phospho-mTOR, leading to inhibition of EOC progression. Furthermore, the pathway was inactivated in SKOV3 cells with the use of a PI3K inhibitor, resulting in EMT inhibition. Thus, we provide evidence that KDM2A may promote EMT through activation of the PI3K/AKT/mTOR pathway in EOC cells.

In summary, the present study demonstrated several roles of KDM2A in EOC. First, KDM2A was overexpressed in EOC and KDM2A has potential as a prognostic marker of EOC. Second, silencing of KDM2A was able to suppress proliferation, migration, invasion and EMT, as well as promote apoptosis in EOC. Additionally, we gained insight into the potential mechanism and showed that KDM2A regulated EMT and the PI3K/AKT/mTOR signaling pathway involved in metastasis. Although there were some notable discoveries in this study, many limitations still exist. One is PCR and animal experiments were not implemented. Although some researchers have confirmed changes of KDM2A expression in other tumors *in vivo* and *in vitro* (11), the results may be different. We demonstrated the effects of PI3K inhibitors in ovarian cancer, but we did not observe the consequence after the treatment of AKT and mTOR inhibitors. Despite these limitations, these results show that KDM2A may serve as a therapeutic target for clinical treatments of EOC patients. Finally, evidence suggests a correlation between EMT and the characteristics of embryonic neural cells, emphasizing the significance of the epigenetic modification enzyme enhancer (41,42). Thus, KDM2A could cause neural development and this behavior may be associated with tumorigenesis.

Acknowledgements

Not applicable.

Funding

No funding was received.

Availability of data and materials

The datasets used during the present study are available from the correspongding author upon reasonable request.

Authors' contributions

DHL, JY, LH and LKG conceived and designed the study. DHL, JM and YL prepared the experimental materials and performed the *in vitro* assays. JC, JMT and MH performed

the bioinformatics study and the data interpretation. DHL, LH, JMT and STL performed the statistical analysis. DHL, LH and MH wrote the manuscript. STL, YL, MH and LH reviewed and edited the manuscript. All authors read and approved the manuscript and agree to be accountable for all aspects of the research in ensuring that the accuracy or integrity of any part of the work are appropriately investigated and resolved.

Ethics approval and consent to participate

Before conducting the scientific investigation, the consent was obtained from all the patients and the study was approved by the Ethics Committee of Wuhan University (Wuhan, China).

Patient consent for publication

Not applicable.

Competing interests

The authors state that they have no competing interests.

References

1. Siegel RL, Miller KD and Jemal A: Cancer statistics, 2016. CA Cancer J Clin 66: 7-30, 2016.
2. Torre LA, Bray F, Siegel RL, Ferlay J, Lortet-Tieulent J and Jemal A: Global cancer statistics, 2012. CA Cancer J Clin 65: 87-108, 2015.
3. Auersperg N: Ovarian surface epithelium as a source of ovarian cancers: Unwarranted speculation or evidence-based hypothesis? Gynecol Oncol 130: 246-251, 2013.
4. Holschneider CH and Berek JS: Ovarian cancer: Epidemiology, biology, and prognostic factors. Semin Surg Oncol 19: 3-10, 2000.
5. Marsden DE, Friedlander M and Hacker NF: Current management of epithelial ovarian carcinoma: A review. Semin Surg Oncol 19: 11-19, 2000.
6. Lengyel E: Ovarian cancer development and metastasis. Am J Pathol 177: 1053-1064, 2010.
7. Shi Y and Whetstine JR: Dynamic regulation of histone lysine methylation by demethylases. Mol Cell 25: 1-14, 2007.
8. Klose RJ and Zhang Y: Regulation of histone methylation by demethylimination and demethylation. Nat Rev Mol Cell Biol 8: 307-318, 2007.
9. Faundes V, Newman WG, Bernardini L, Canham N, Clayton-Smith J, Dallapiccola B, Davies SJ, Demos MK, Goldman A, Gill H, *et al*: Histone lysine methylases and demethylases in the landscape of human developmental disorders. Am J Hum Genet 102: 175-187, 2018.
10. Tsukada Y, Fang J, Erdjument-Bromage H, Warren ME, Borchers CH, Tempst P and Zhang Y: Histone demethylation by a family of JmjC domain-containing proteins. Nature 439: 811-816, 2006.
11. Wagner KW, Alam H, Dhar SS, Giri U, Li N, Wei Y, Giri D, Cascone T, Kim JH, Ye Y, *et al*: KDM2A promotes lung tumorigenesis by epigenetically enhancing ERK1/2 signaling. J Clin Invest 123: 5231-5246, 2013.
12. Nalla AK, Williams TF, Collins CP, Rae DT and Trobridge GD: Lentiviral vector-mediated insertional mutagenesis screen identifies genes that influence androgen independent prostate cancer progression and predict clinical outcome. Mol Carcinog 55: 1761-1771, 2016.
13. Cao LL, Du C, Liu H, Pei L, Qin L, Jia M and Wang H: Lysine-specific demethylase 2A expression is associated with cell growth and cyclin D1 expression in colorectal adenocarcinoma. Int J Biol Markers 1: 1724600818764069, 2018.
14. Chen JY, Luo CW, Lai YS, Wu CC and Hung WC: Lysine demethylase KDM2A inhibits TET2 to promote DNA methylation and silencing of tumor suppressor genes in breast cancer. Oncogenesis 6: e369, 2017.
15. Kong Y, Zou S, Yang F, Xu X, Bu W, Jia J and Liu Z: RUNX3-mediated up-regulation of miR-29b suppresses the proliferation and migration of gastric cancer cells by targeting KDM2A. Cancer Lett 381: 138-148, 2016.
16. Zhu L, Li Q, Wong SH, Huang M, Klein BJ, Shen J, Ikenouye L, Onishi M, Schneidawind D, Buechele C, *et al*: ASH1L links histone H3 lysine 36 dimethylation to MLL leukemia. Cancer Discov 6: 770-783, 2016.
17. Chen JY, Li CF, Chu PY, Lai YS, Chen CH, Jiang SS, Hou MF and Hung WC: Lysine demethylase 2A promotes stemness and angiogenesis of breast cancer by upregulating Jagged1. Oncotarget 7: 27689-27710, 2016.
18. Bowen NJ, Walker LD, Matyunina LV, Logani S, Totten KA, Benigno BB and McDonald JF: Gene expression profiling supports the hypothesis that human ovarian surface epithelia are multipotent and capable of serving as ovarian cancer initiating cells. BMC Med Genomics 2: 71, 2009.
19. Ritchie ME, Phipson B, Wu D, Hu Y, Law CW, Shi W and Smyth GK: limma powers differential expression analyses for RNA-sequencing and microarray studies. Nucleic Acids Res 43: e47, 2015.
20. Ito K and Murphy D: Application of ggplot2 to Pharmacometric Graphics. CPT Pharmacometrics Syst Pharmacol 2: e79, 2013.
21. Hu J, Meng Y, Zhang Z, Yan Q, Jiang X, Lv Z and Hu L: MARCH5 RNA promotes autophagy, migration, and invasion of ovarian cancer cells. Autophagy 13: 333-344, 2017.
22. Li Y, Wu T, Wang Y, Yang L, Hu C, Chen L and Wu S: γ-Glutamyl cyclotransferase contributes to tumor progression in high grade serous ovarian cancer by regulating epithelial-mesenchymal transition via activating PI3K/AKT/mTOR pathway. Gynecol Oncol 149: 163-172, 2018.
23. Jiang Y, Qian X, Shen J, Wang Y, Li X, Liu R, Xia Y, Chen Q, Peng G, Lin SY and Lu Z: Local generation of fumarate promotes DNA repair through inhibition of histone H3 demethylation. Nat Cell Biol 17: 1158-1168, 2015.
24. Huang Y, Liu Y, Yu L, Chen J, Hou J, Cui L, Ma D and Lu W: Histone demethylase KDM2A promotes tumor cell growth and migration in gastric cancer. Tumour Biol 36: 271-278, 2015.
25. Naora H and Montell DJ: Ovarian cancer metastasis: Integrating insights from disparate model organisms. Nat Rev Cancer 5: 355-366, 2005.
26. Shield K, Ackland ML, Ahmed N and Rice GE: Multicellular spheroids in ovarian cancer metastases: Biology and pathology. Gynecol Oncol 113: 143-148, 2009.
27. Yilmaz M and Christofori G: EMT, the cytoskeleton, and cancer cell invasion. Cancer Metastasis Rev 28: 15-33, 2009.
28. Kotiyal S and Bhattacharya S: Breast cancer stem cells, EMT and therapeutic targets. Biochem Biophys Res Commun 453: 112-116, 2014.
29. Nieto MA, Huang RY, Jackson RA and Thiery JP: EMT: 2016. Cell 166: 21-45, 2016.
30. van Roy F and Berx G: The cell-cell adhesion molecule E-cadherin. Cell Mol Life Sci 65: 3756-3788, 2008.
31. Christofori G and Semb H: The role of the cell-adhesion molecule E-cadherin as a tumour-suppressor gene. Trends Biochem Sci 24: 73-76, 1999.
32. Berx G, Cleton-Jansen AM, Nollet F, de Leeuw WJ, van de Vijver M, Cornelisse C and van Roy F: E-cadherin is a tumour/invasion suppressor gene mutated in human lobular breast cancers. EMBO J 14: 6107-6115, 1995.
33. Pećina-Slaus N: Tumor suppressor gene E-cadherin and its role in normal and malignant cells. Cancer Cell Int 3: 17, 2003.
34. Duran GE, Wang YC, Moisan F, Francisco EB and Sikic BI: Decreased levels of baseline and drug-induced tubulin polymerisation are hallmarks of resistance to taxanes in ovarian cancer cells and are associated with epithelial-to-mesenchymal transition. Br J Cancer 116: 1318-1328, 2017.
35. Cheng YC, Tsao MJ, Chiu CY, Kan PC and Chen Y: Magnolol inhibits human glioblastoma cell migration by regulating N-cadherin. J Neuropathol Exp Neurol 77: 426-436, 2018.
36. Liu N, Peng SM, Zhan GX, Yu J, Wu WM, Gao H, Li XF and Guo XQ: Human chorionic gonadotropin β regulates epithelial-mesenchymal transition and metastasis in human ovarian cancer. Oncol Rep 38: 1464-1472, 2017.

37. Colomiere M, Ward AC, Riley C, Trenerry MK, Cameron-Smith D, Findlay J, Ackland L and Ahmed N: Cross talk of signals between EGFR and IL-6R through JAK2/STAT3 mediate epithelial-mesenchymal transition in ovarian carcinomas. Br J Cancer 100: 134-144, 2009.
38. Lamouille S, Xu J and Derynck R: Molecular mechanisms of epithelial-mesenchymal transition. Nat Rev Mol Cell Biol 15: 178-196, 2014.
39. Cheaib B, Auguste A and Leary A: The PI3K/Akt/mTOR pathway in ovarian cancer: Therapeutic opportunities and challenges. Chin J Cancer 34: 4-16, 2015.
40. Sain N, Krishnan B, Ormerod MG, De Rienzo A, Liu WM, Kaye SB, Workman P and Jackman AL: Potentiation of paclitaxel activity by the HSP90 inhibitor 17-allylamino-17-demethoxygeldanamycin in human ovarian carcinoma cell lines with high levels of activated AKT. Mol Cancer Ther 5: 1197-1208, 2006.
41. Cao Y: Tumorigenesis as a process of gradual loss of original cell identity and gain of properties of neural precursor/progenitor cells. Cell Biosci 7: 61, 2017.
42. Zhang Z, Lei A, Xu L, Chen L, Chen Y, Zhang X, Gao Y, Yang X, Zhang M and Cao Y: Similarity in gene-regulatory networks suggests that cancer cells share characteristics of embryonic neural cells. J Biol Chem 292: 12842-12859, 2017.